Available online at www.sciencedirect.com
SCIENCE DIRECT®
Journal of Solid State Chemistry 173 (2003) 456–461
JOURNAL OF SOLID STATE CHEMISTRY
http://elsevier.com/locate/jssc

Charge disorder effects in 3*d* transition metal oxide perovskites

A.J. Williams,[a,b] B.M. Sobotka,[a,b] and J.P. Attfield[a,b,*]

[a] *Department of Chemistry, University of Cambridge, Lensfield Road, Cambridge CB2 1EW, UK*
[b] *Interdisciplinary Research Centre in Superconductivity, University of Cambridge, Madingley Road, Cambridge CB3 0HE, UK*

Received 15 August 2002; received in revised form 15 November 2002; accepted 21 November 2002

Abstract

The effects of the random electrostatic potential due to differences in formal charge between *A* site R^{3+} (lanthanide, Y), M^{2+} (Ca, Sr, Ba) and Th^{4+} cations have been investigated in ferromagnetic $AMnO_3$ and superconducting A_2CuO_4 perovskites. Series of samples in which the mean *A* site charge and the mean and variance of the *A* cation radius distribution are held constant, but the *A* site charge variance increases, show no significant changes of the electronic (Curie or superconducting) transition temperatures. The effect of the *A* cation random potentials on electronic transitions in the 3*d* metal oxide perovskites are insignificant in comparison to the lattice effects from the differing cation sizes.

Keywords: Manganese oxide; Perovskites; Cuprate super-conductors; Charge variance; Random potentials; Lattice effects

1. Introduction

The effects of disorder in crystalline electronic conductors and superconducting materials have been investigated theoretically and experimentally for many years. Early free-electron theories showed that a small randomness in periodic potential amplitudes leads to electron trapping in localized states [1], and can lead to an Anderson-type metal-to-insulator transition [2]. Non-magnetic random scattering does not affect conventional *s*-wave superconductors [3], but may lead to a strong suppression of the superconducting transition in some recent approaches to *d*-wave superconductivity in the high-T_c cuprates [4].

Perovskite oxides offer many opportunities to study the effects of random potentials in exotic conductors, as the conducting state is often generated by chemical doping of a parent oxide. The representative materials that will be considered in this study are the pseudo-cubic manganite perovskites $AMnO_3$, e.g., $La_{0.7}Sr_{0.3}MnO_3$, that have a ferromagnetic metallic ground state stabilized by the double-exchange interaction [5,6], and layered A_2CuO_4 cuprates, e.g., $La_{1.85}Sr_{0.15}CuO_4$ that are superconducting at low temperatures [7]. Many substitutions of R^{3+} (= rare earth, Y) and M^{2+} (= Ca, Sr, Ba) cations are possible at the *A* sites, enabling the influence of the *A* cation mixture on the physical properties of the transition metal (*T*) oxide network to be elucidated. In the simplest approximation, the *A* cations are described as hard spheres with characteristic radii (*r*) and integral charges (*q*). The primary electronic control of the *A* cations is through the doping concentration $\langle q_A \rangle - q_A^0.\langle q_A \rangle$ is the mean *A* site charge ($\langle\ \rangle$ denotes an average throughout) and q_A^0 (= 3 in both systems) is the charge in the undoped material. The lattice effects of the *A* cations are traditionally quantified by the mean A cation radius $\langle r_A \rangle$, which is often represented through the perovskite tolerance factor, $t = (\langle r_A \rangle + r_O)/\sqrt{2}(r_T + r_O)$. The electronic transition temperatures are a sensitive measure of changing electronic or lattice effects, and they generally decrease as $\langle r_A \rangle$ decreases. However, recent studies have shown that the *A* cation size mismatch is of comparable influence, and this is conveniently quantified through the variance (second moment) of the *A* cation radius distribution $\sigma^2(r_A) = \langle r_A^2 \rangle - \langle r_A \rangle^2$, written as σ^2 in previous studies [8–13].

The importance of $\sigma^2(r_A)$ was demonstrated by using mixtures of several *A* cations in series of $(R_{1-x}M_x)MnO_3$ perovskites for which the doping level (and hence $\langle q_A \rangle$) was fixed at $x = 0.3$, and the mean radius $\langle r_A \rangle$ was

*Corresponding author. Department of Chemistry, University of Cambridge, Lensfield Road, Cambridge CB2 1EW, UK. Fax: +44-1223-336362.
E-mail address: jpa14@cam.ac.uk (J.P. Attfield).

0022-4596/03/$ - see front matter © 2003 Elsevier Science (USA). All rights reserved.
doi:10.1016/S0022-4596(03)00012-4

also fixed, but $\sigma^2(r_A)$ was varied systematically [8–11]. T_m, the metal–insulator transition temperature that coincides with the ferromagnetic Curie temperature T_C, shows a linear decrease with increasing $\sigma^2(r_A)$, from 360 to 100 K in one series [8]. A linear decrease of the superconducting transition temperature T_c with $\sigma^2(r_A)$ in $R_{1.85}M_{0.15}CuO_4$ at constant $\langle r_A \rangle$ was also observed [12,13]. A strong linear increase of structural phase transitions with $\sigma^2(r_A)$ was found in the latter $R_{1.85}M_{0.15}CuO_4$ series [13] and for the ferroelectric Curie temperature in doped $BaTiO_3$ [14]. Although a full theoretical treatment of the $\sigma^2(r_A)$ effects has not been produced, an empirical approach has proposed that $\sigma^2(r_A)$ describes the coupling of the various transitions to a long-range incoherent strain arising from static structural fluctuations [15]. The corresponding coherent strain arising from the A cation mixture is then proportional to $(\langle r_A \rangle - r_A^0)^2$; together with $\sigma^2(r_A)$ this gives a reasonably quantitative description for the variation of T_m between many $(R_{0.7}M_{0.3})MnO_3$ compositions [11].

The mixing of R^{3+} and M^{2+} produces a charge disorder described by the A cation charge variance $\sigma^2(q_A) = \langle q_A^2 \rangle - \langle q_A \rangle^2$ in addition to the incoherent strain $\sigma^2(r_A)$. $\sigma^2(q_A)$ parameterizes the random electrostatic potential from the A cations acting on the charge carriers in the transition metal oxide framework. When $A = (R^{3+}_{1-x}M^{2+}_x)$, $\sigma^2(q_A) = x \cdot (1-x)$ so the maximum $\sigma^2(q_A) = 0.25$ is at $x = 0.5$. For a cubic $(R^{3+}_{0.5}M^{2+}_{0.5})TO_3$ perovskite with cell constant $a_p \sim 4$ Å, this corresponds to a root mean square fluctuation of ~ 2.0 eV in the electrostatic potential energy of an electron at the T site, due to the eight nearest A cations, which is comparable to the 3d-band widths. In reality, the local charges will be reduced from the formal ionic values, however, the remaining random A cation potential will scale as $\sigma^2(q_A)$.

To determine whether $\sigma^2(q_A)$ has a significant influence on the electronic transition temperatures of manganites and cuprates, we have prepared a series of perovskites in which known important factors ($\langle q_A \rangle$, $\langle r_A \rangle$, and $\sigma^2(r_A)$) are held constant while $\sigma^2(q_A)$ changes systematically. This is done by progressively substituting R^{3+} with a 1:1 mixture of M^{2+} and Th^{4+}. The radius of Th^{4+} (1.09 Å) is comparable to that of the smaller lanthanides and Y^{3+} (1.075 Å) (all radius calculations use nine-coordinate ionic radii from [16]). Randomization of any residual lattice effects is achieved by varying some of the R^{3+} or M^{2+} cations between samples, so that any remaining trends in the measured transition temperatures are a true reflection of the changing $\sigma^2(q_A)$.

2. Experimental

For comparison with previous experiments on $\sigma^2(r_A)$ effects, 30% doped $AMnO_3$ and 15% doped A_2CuO_4 compositions have been prepared as polycrystalline powders. The manganites (Table 1) have a fixed $\langle r_A \rangle = 1.255$ Å and $\sigma^2(r_A) = 0.019$ Å^2 and were prepared by solid-state reaction in air at 1500°C followed by quenching to room temperature. The cuprates (Table 2) have $\langle r_A \rangle = 1.223$ Å and $\sigma^2(r_A) = 0.002$ Å^2 and were prepared by solid-state reaction in air at 1050°C, then annealed at 400°C in flowing oxygen. The experimental maxima of $\sigma^2(q_A)$ were determined by the solubility limits of Th^{4+}, which were 7.5% in the manganites and

Table 1
A cation composition, charge variance and measured properties for a series of 30% doped $AMnO_3$ perovskites with fixed $\langle r_A \rangle = 1.255$ Å and $\sigma^2(r_A) = 0.019$ Å^2

A site composition	$\sigma^2(q_A)$	Oxygen content	a (Å)	b (Å)	c (Å)	T_C (K)	θ (K)
$Pr_{0.62}Y_{0.08}Sr_{0.02}Ba_{0.28}$	0.21	3.00(1)	5.4953(1)	7.7623(1)	5.5122(1)	123	170
$Pr_{0.1}Nd_{0.55}Sr_{0.045}Th_{0.025}Ba_{0.28}$	0.26	3.00(2)	5.4888(2)	7.7632(2)	5.5141(1)	150	158
$La_{0.45}Y_{0.15}Ca_{0.05}Sr_{0.05}Th_{0.05}Ba_{0.25}$	0.31	2.97(2)	5.4969(1)	7.7788(2)	5.5136(1)	130	176
$Nd_{0.55}Sr_{0.11}Th_{0.075}Ba_{0.265}$	0.36	2.99(1)	5.4897(1)	7.7651(2)	5.5113(1)	137	164

Table 2
A cation composition, charge variance and measured properties for a series of 15% doped A_2CuO_4 perovskites with fixed $\langle r_A \rangle = 1.223$ Å and $\sigma^2(r_A) = 0.002$ Å^2

A site composition	$\sigma^2(q_A)$	Oxygen content	a (Å)	c (Å)	Onset T_c (K)	Bulk T_c (K)
$La_{0.859}Nd_{0.066}Ba_{0.022}Sr_{0.053}$	0.069	4.01(4)	3.7787(1)	13.2192(3)	24.3	11.1
$La_{0.896}Gd_{0.028}Th_{0.001}Ba_{0.019}Sr_{0.058}$	0.071	4.04(4)	3.7792(1)	13.2189(3)	24.0	11.9
$La_{0.889}Eu_{0.031}Th_{0.003}Ba_{0.019}Sr_{0.059}$	0.074	4.02(4)	3.7819(1)	13.2034(4)	19.8	10.4
$La_{0.829}Pr_{0.086}Th_{0.005}Ba_{0.021}Sr_{0.059}$	0.079	4.05(4)	3.7779(1)	13.2152(3)	27.4	25.2
$La_{0.876}Sm_{0.029}Th_{0.01}Ba_{0.017}Sr_{0.068}$	0.089	3.98(4)	3.7790(1)	13.2176(4)	24.3	17.3
$La_{0.854}Nd_{0.041}Th_{0.015}Ba_{0.016}Sr_{0.074}$	0.099	3.97(4)	3.7789(1)	13.2261(4)	27.8	26.2

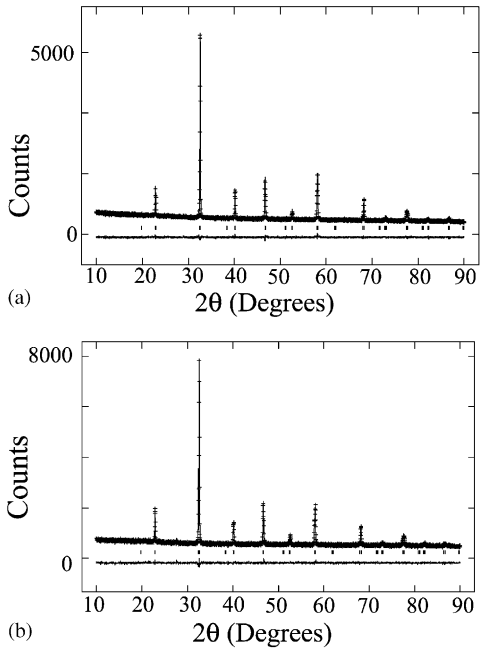

Fig. 1. Observed, calculated and difference X-ray diffraction data for representative manganite samples: (a) $Pr_{0.62}Y_{0.08}Sr_{0.02}Ba_{0.28}MnO_3$, $\sigma^2(q_A) = 0.21$; (b) $Nd_{0.55}Sr_{0.11}Th_{0.075}Ba_{0.265}MnO_3$, $\sigma^2(q_A) = 0.36$.

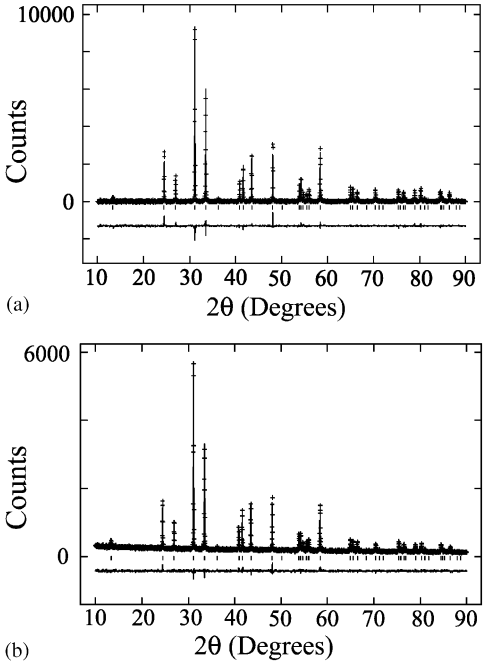

Fig. 2. Observed, calculated and difference X-ray diffraction patterns for representative cuprate samples: (a) $(La_{0.859}Nd_{0.066}Ba_{0.022}Sr_{0.053})_2CuO_4$, $\sigma^2(q_A) = 0.069$; (b) $(La_{0.854}Nd_{0.041}Th_{0.015}Ba_{0.016}Sr_{0.074})_2CuO_4$, $\sigma^2(q_A) = 0.099$.

1.5% for the cuprates. Single-phase samples (by X-ray powder diffraction, see Figs. 1 and 2) were obtained below these limits. Although the limits of Th substitution are small, they represent increases in $\sigma^2(q_A)$ of 70% for the manganites and 40% for the cuprates over the minimum value in the first, Th-free, $(R^{3+}_{1-x}M^{2+}_x)$ composition, giving a sufficient range for any strong trends with $\sigma^2(q_A)$ to be observed.

X-ray powder diffraction patterns were Rietveld analyzed using the GSAS program [17] to determine the superstructure types and extract the unit-cell parameters (Table 1). The manganites (Fig. 1) all have the orthorhombic $\sqrt{2}a_p \times 2a_p \times \sqrt{2}a_p$ Imma superstructure, consistent with their position in the chemical window for 30% doped $AMnO_3$ perovskites [11]. The cuprates (Fig. 2) all have the tetragonal $I4/mmm$ La_2CuO_4-type structure. Oxygen contents (Table 1), measured by iodometric titrations for the manganites and by thermogravimetry for the cuprates, did not change significantly with $\sigma^2(q_A)$. Magnetizations were measured using a SQUID magnetometer.

3. Results and discussion

The four manganite samples exhibit sharp ferromagnetic transitions in the magnetization/field (M/H) data (Fig. 3(a)) at 123–150 K. T_C was obtained from the

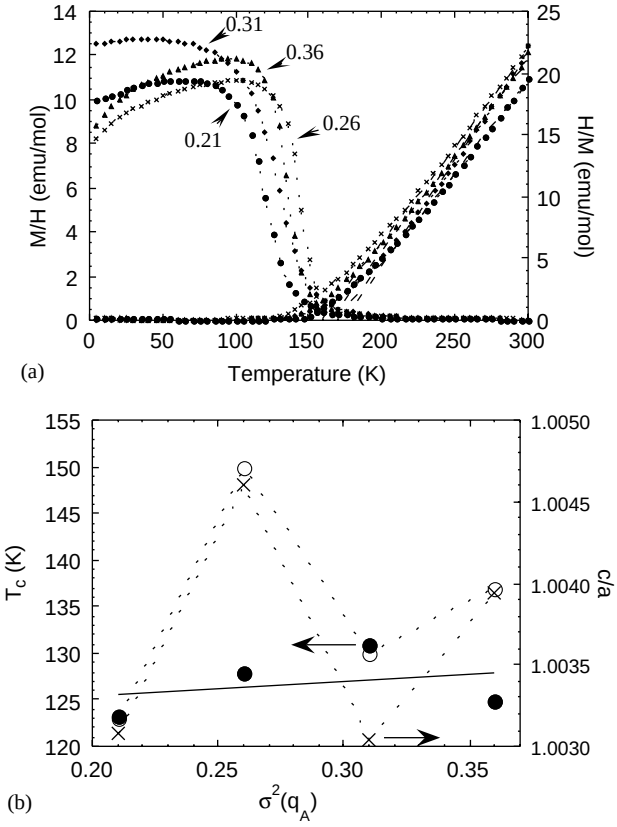

Fig. 3. Results for the manganites listed in Table 1. (a) Molar M/H and H/M vs temperature with $\sigma^2(q_A)$ values labeled. Data were measured at H = 500 Oe. (b) Plot of measured T_C (open circles), scaled T_C (filled circles) and the c/a cell parameter ratio (crosses) against $\sigma^2(q_A)$. A linear fit to the scaled T_C points is shown, the other data are connected point to point as a guide to the eye.

minimum in $d(M/H)/dT$ (this is not a thermodynamically correct definition, but it is widely used and provides a robust value for comparison of cubic manganites [9]), and the Weiss constant, θ, was estimated from a linear fit to the H/M in the paramagnetic regime for each sample. The variation of θ (Table 1) shows a negative correlation with T_C, which suggests that the upper measurement temperature of 300 K is not sufficiently far above T_C to give accurately extrapolated θ values. The T_C values show no significant trend with $\sigma^2(q_A)$ (Fig. 3(b)) but significant sample-to-sample variations in T_C are observed. These did not correlate with possible additional factors such as A cation masses or magnetic moments, but did correlate strongly with the c/a ratio of unit-cell parameters, which are also plotted in Fig. 3(b). To allow for this small residual variation in lattice effects, the T_C's were scaled relative to the value of the first ($\sigma^2(q_A) = 0.21$) sample using a linear scaling between T_C and c/a. The scaled T_C values (Fig. 1(b)) of 123–131 K are not significantly different from each other and show no trend with $\sigma^2(q_A)$. The experimental errors of ± 4 K over the experimental range of $\sigma^2(q_A)$ give the upper bound of $|dT_C/d\sigma^2(q_A)|$ to be 25 K. Hence, the maximum possible suppression of the Curie temperature arising from A cation charge disorder in a $(R^{3+}_{1-x}M^{2+}_x)MnO_3$ material (at $x = 0.5$) is estimated as 7 K. This is small compared to the maximum T_C of 360 K in the cubic manganites.

The six cuprate samples all show a superconducting transition below 30 K (Fig. 4(a)) but show varying minimum diamagnetic susceptibilities. These do not correlate with $\sigma^2(q_A)$ and may reflect variations in grain growth due to the different A cation mixtures. Onset T_c's were taken as the onset of deviation of the measured magnetization from zero (Fig. 4(b)), and bulk T_c's were estimated from the crossover of the extrapolated maximum slope with the zero magnetization axis. The onset T_c's show no trend with $\sigma^2(q_A)$, but do show significant variations between samples. These variations were again found to correlate with the lattice parameters, shown as the c/a ratio in Fig. 4(b). In particular,

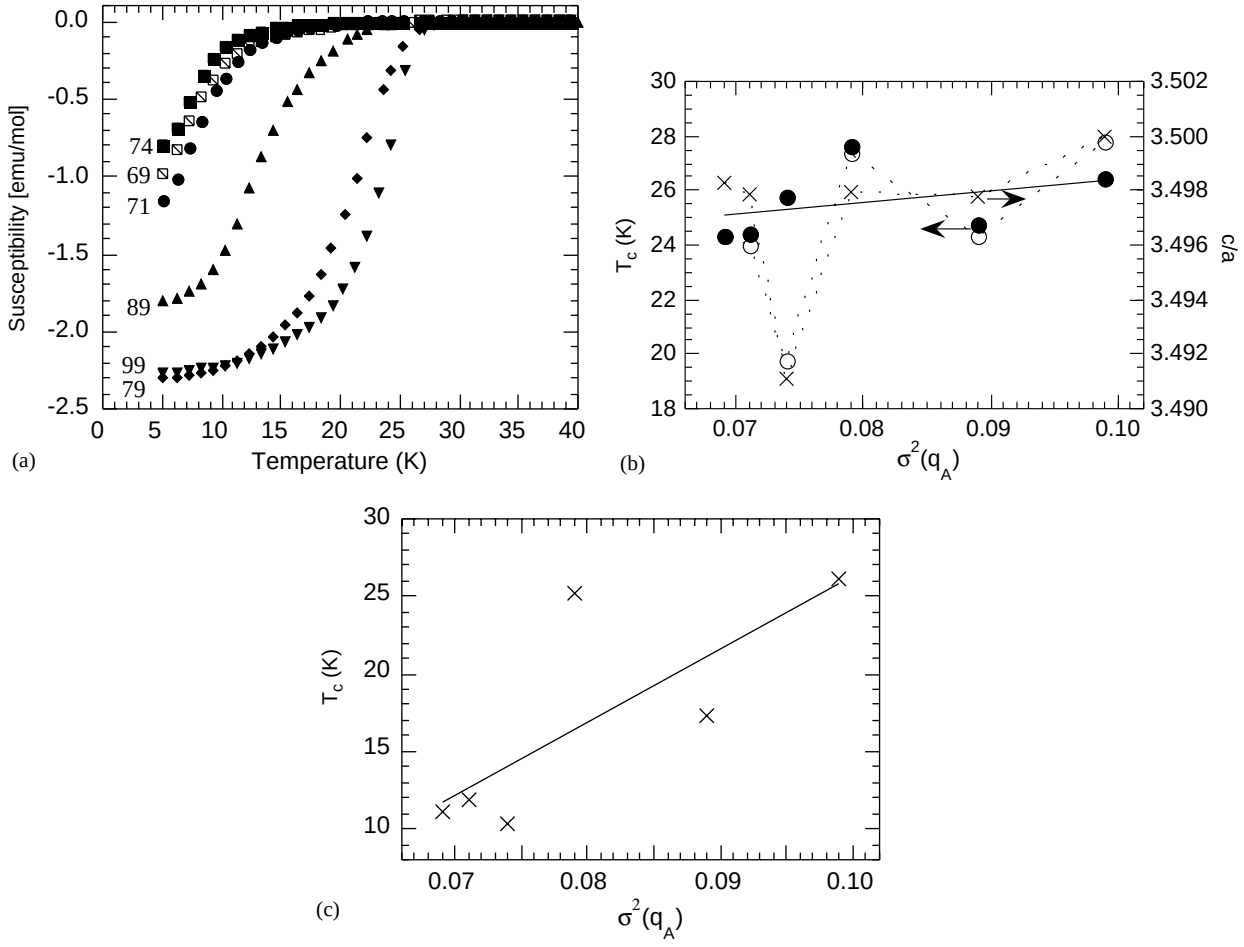

Fig. 4. Results for the cuprates listed in Table 2. (a) Temperature dependence of the magnetic susceptibility, measured on warming in a 20 Oe field after zero field cooling, with $\sigma^2(q_A)$ values ($\times 10^3$) labeled (b) Plot of measured onset T_c (open circles), scaled onset T_c (filled circles) and the c/a cell parameter ratio (crosses) against $\sigma^2(q_A)$. A linear fit to the scaled T_c points is shown, the other data are connected point to point as a guide to the eye. (c) Plot of bulk T_c against $\sigma^2(q_A)$ with a linear fit.

outlying low values of both T_c and c/a are found for the third ($\sigma^2(q_A) = 0.074$) sample. These T_c values were scaled relative to the value for the first sample using a linear scaling with c/a, as for the manganites. The scaled onset T_c's all lie in a narrow range of 24–28 K and show no trend with $\sigma^2(q_A)$. However, the bulk T_c's (Fig. 4(c)) show a much wider dispersion and an apparent increase in T_c with $\sigma^2(q_A)$. This is unphysical and suggests that some of the cuprate samples are inhomogeneous superconductors. Experiments on other samples over a wider range of $\sigma^2(q_A)$ would be needed to find a possible $\sigma^2(q_A)$ dependence in the cuprates.

The small observed variations in the transition temperatures result from variations in lattice or chemical effects in both the manganites and cuprates, despite the samples having the same $\langle r_A \rangle$ and $\sigma^2(r_A)$ values. This reflects experimental uncertainties in the ionic radii which are typically accurate to ± 0.005 Å [16], as well as the limits of the present approximation for parameterizing lattice effects. $\sigma^2(q_A)$, is found to cause no significant suppression on the transition temperatures of the ferromagnetic manganites or the superconducting cuprates over the range of $\sigma^2(q_A)$ values found in typical $A = (R_{1-x}M_x)$ compositions.

The only previous study to consider the effects of $\sigma^2(q_A)$ was a comparison of the $(Sr_{1-x}Ca_x)RuO_3$ and $(Sr_{1-x}(Na_{0.5}La_{0.5})_x)RuO_3$ systems [18]. Although the lattice effects from $\langle r_A \rangle$ and $\sigma^2(r_A)$ are greater in the former series, ferromagnetism is more rapidly suppressed with x in the latter, and this was ascribed to the large increase up to $\sigma^2(q_A) = 1.0$ at $x = 1$ present only in the second system. The apparently greater sensitivity of the 3d manganese and copper oxides to lattice effects, and the smaller available ranges of $\sigma^2(q_A)$, result in any charge disorder effects being unimportant in the latter systems. It would be interesting to study the effects of $\sigma^2(r_A)$ and $\sigma^2(q_A)$ systematically in the 4d ruthenates for comparison with the 3d transition metal oxides.

Both the A cation size and charge variances, $\sigma^2(r_A)$ and $\sigma^2(q_A)$, parameterize random fields that have length scales of $\sim a_p$ (≈ 4 Å) in conducting perovskite oxides. This is comparable to the mean free path for electronic conduction in manganites [19] and the coherence length ξ in cuprate superconductors. (ξ is strongly anisotropic; at $T \to 0$, $\xi_c \sim 1$ Å and $\xi_{ab} \sim 14$ Å [20]). However, $\sigma^2(r_A)$ leads to a strong suppression of the Curie or superconducting transition (at constant $\langle q_A \rangle$, $\langle r_A \rangle$ and $\sigma^2(q_A)$) whereas no measurable suppression with $\sigma^2(q_A)$ has been observed in this study (at constant $\langle q_A \rangle$, $\langle r_A \rangle$ and $\sigma^2(r_A)$). The conductivity or superconductivity results in part from strong hybridization between T:3d_σ and O:2p_σ orbitals, which is very sensitive to the T–O distances and T–O–T angles. Diffraction studies have confirmed that local variations in both the distances and angles increase with $\sigma^2(r_A)$ [21,22], although the mean values also change slightly as $\sigma^2(r_A)$ couples to the overall lattice strain.

4. Conclusions

$\sigma^2(q_A)$ describes effects from the random A cation electrostatic potential upon the charge carriers in the transition metal oxide framework that are independent of the lattice effects. This study has shown that it is very difficult to hold lattice and other chemical factors constant between different samples to look for $\sigma^2(q_A)$ effects. Fixing $\langle r_A \rangle$ and $\sigma^2(r_A)$ produces samples with lattice parameters that are constant to $\sim 0.2\%$ and show no systematic dependence on $\sigma^2(q_A)$. However, these variations are still sufficient to produce measurable differences in the Curie temperatures of the manganites and after an empirical scaling to correct for the residual lattice effects, no significant dependence upon $\sigma^2(q_A)$ is observed. This demonstrates that local charge variations are very effectively screened in doped 3d metal oxides, so that random A cation potentials have no significant effect on the electronic transitions.

Acknowledgments

The authors thank Dr. J.A. McAllister and Dr. G. Corbel for their assistance with the magnetic measurements. A.J.W. acknowledges EPSRC and Rutherford–Appleton Laboratory for support and B.M.S. acknowledges the German Academic Exchange Service (DAAD) for a scholarship.

References

[1] P.W. Anderson, Phys. Rev. 109 (1958) 1492.
[2] N.F. Mott, Philos. Mag. 13 (1966) 989.
[3] P.W. Anderson, J. Phys. Chem. Solids 11 (1959) 26.
[4] R.J. Radtke, K. Levin, H.B. Schuttler, M.R. Norman, Phys. Rev. B 48 (1993) 653;
L.S. Borkowski, P.J. Hirschfeld, Phys. Rev. B 49 (1994) 15404.
[5] Z. Jirak, E. Pollert, A.F. Andersen, J.C. Grenier, P. Hagenmuller, Eur. J. Solid State Inorg. Chem. 27 (1990) 421.
[6] H.Y. Hwang, S.W. Cheong, P.G. Radaelli, M. Marezio, B. Batlogg, Phys. Rev. Lett. 75 (1995) 914.
[7] J.G. Bednorz, K.A. Muller, Z. Phys. B 64 (1986) 189.
[8] L.M. Rodriguez-Martinez, J.P. Attfield, Phys. Rev. B 54 (1996) R15622.
[9] L.M. Rodríguez-Martínez, H. Ehrenberg, J.P. Attfield, J. Solid State Chem. 148 (1999) 20.
[10] L.M. Rodríguez-Martínez, H. Ehrenberg, J.P. Attfield, Solid State Sci. 1 (2000) 11.
[11] L.M. Rodriguez-Martinez, J.P. Attfield, Phys. Rev. B 63 (2000) 24424.
[12] J.P. Attfield, A.L. Kharlanov, J.A. McAllister, Nature 394 (1998) 157.
[13] J.A. McAllister, J.P. Attfield, Phys. Rev. Lett. 83 (1999) 3289.

[14] D.C. Sinclair, J.P. Attfield, Chem. Commun. 16 (1999) 1497.
[15] J.P. Attfield, Chem. Mater. 10 (1998) 3239.
[16] R.D. Shannon, Acta Crystallogr. A 32 (1976) 751.
[17] A.C. Larson, R.B. von Dreele, GSAS: General Structure Analysis System, LANSCE, MS-H805, Los Alamos National Laboratory, Los Alamos, NM, 1994.
[18] T. He, Q. Huang, R.J. Cava, Phys. Rev. B 63 (2001) 24402.
[19] Y. Sawaki, K. Takenaka, A. Osuka, R. Shiozaki, S. Sugai, Phys. Rev. B 61 (2000) 11588.
[20] W.C. Lee, R.A. Klemm, D.C. Johnston, Phys. Rev. B 63 (1989) 1012.
[21] L.M. Rodríguez-Martínez, J.P. Attfield, Phys. Rev. B 58 (1998) 2426.
[22] J.A. McAllister, J.P. Attfield, Phys. Rev. B 66 (2002) 14514.